

SORPTION OF Eu(III) ON QUARTZ AT HIGH SALT CONCENTRATIONS

David García^{a,*}, Johannes Lützenkirchen^{b,*}, Vladimir Petrov^{c,*}, Matthieu Siebentritt^d, Dieter Schild^b, Grégory Lefèvre^d, Thomas Rabung^b, Marcus Altmaier^b, Stepan Kalmykov^c, Lara Duro^b, Horst Geckeis^b

a. Amphos 21, Carrer Veneçuela 103, 08019, Barcelona (ES)

b. Karlsruhe Institute of Technology (KIT) Institut für Nukleare Entsorgung (INE) ,Hermann-von-Helmholtz-Platz 1, 76344 Eggenstein-Leopoldshafen (GER)

c. Lomonosov Moscow State University, Department of Chemistry, Leninskie gory, 1/3, 119991, Moscow (RU)

d. PSL Research University, Chimie ParisTech — CNRS, Institut de Recherche de Chimie Paris, 75005, Paris, France (FR)

Abstract

Sorption of Eu(III) onto quartz from highly saline solutions (up to 5M NaCl) has been studied by sorption edges. The acid-base titrations of the solid surface suggest the rather unusual presence of two different sites that has been the object of recent discussions in the literature. Europium uptake results show the usual behaviour with a steep pH-edge and nearly complete removal at sufficiently high pH. Previous spectroscopic data on this system suggest the presence of two bidentate surface complexes with different proton stoichiometry. Based on this, a self-consistent Surface Complexation Model (SCM) was fitted to the full set of experimental data, from 0.1 to 5 M NaCl, using a coupled Pitzer/surface complexation approach. The Pitzer model was applied to aqueous species. A Basic Stern Model was used for interfacial electrostatics of the system, which includes ion-specific effects via ion-pair formation. Parameter fitting was done using the general parameter estimation software UCODE coupled to a modified version of FITEQL2 involving separate calculations of the respective ionic strength corrections. At high ionic strength (>1 M), the surface potential is strongly screened by ion-pair formation and the diffuse layer potential is negligibly low, which justifies the extension of the standard electrostatic model to these harsh conditions. Overall, our model is able to describe the full set of analysed data. It is expected that these first systematic data acquisition along with the detailed modelling can serve as a benchmark for the modelling of future studies on sorption in highly saline systems.

Keywords

Sorption, radionuclides, silica, high ionic strength, modelling, europium

* Corresponding author: Dr. David García. E-mail: david.garcia@amphos21.com. +34 935 830 500

* Corresponding author: Dr. Johannes Lützenkirchen. E-mail: johannes.luetzenkirchen@kit.edu. +49 721 608-2402

* Corresponding author: Dr. Vladimir Petrov. E-mail: vladimir.g.petrov@gmail.com

1. Introduction

Adsorption processes are important in retarding the potential migration of radionuclides from a nuclear waste repository to the biosphere^{1,2}. Many studies have been carried out to characterize the interactions of key radionuclides on many surfaces for a wide range of solution compositions. The major body of the studies was performed with salt concentrations of 0.1M and below³ and references therein). Surface complexation modelling approaches⁴⁻⁶ have rationalized the adsorption of dissolved ions (such as heavy metal ions or radionuclides) in a fashion similar to the treatment of aqueous complexation equilibria. In particular, on oxides, surface ligands (surface hydroxyl groups) undergo protonation and/or deprotonation which allow, along with an electrostatic model for the interface, the description of the charging curves of the surfaces under study. The fundamental charging of oxide surfaces occurs via proton uptake or release from the surface functional groups. The surface charge is pH dependent and influenced by the electrolyte ions and increases with ionic strength. Adsorption of other solutes like radionuclides is also pH dependent and affected by the variable charge of the surface. For salt concentrations significantly higher than 0.1M there is no systematic data set to allow an extension of the present modelling approaches to higher salt contents within a variable charge model. In one case, data for sorption on montmorillonite were modelled using a combined Pitzer and triple layer approach by Mahoney and Langmuir⁷. In Mahoney and Langmuir study's, the data were more adequately modelled up to 4.0 M NaCl (encompassing data at 1.0 and 2.0 M NaCl for the high concentration range) using activity coefficients calculated by the Davies equation than by using Pitzer based activity coefficient models. It is unclear how the pH measurements were actually done at the high salt level⁸ and if the charges were accurately determined in the high salt level range, a Basic Stern model coupled to the Davies equation was successful in describing the reported data also in 4.0 M NaCl⁹. The situation is different for aqueous solubility and speciation of radionuclides where a large body of systematic experimental data exists. In these cases, SIT and Pitzer modelling approaches set thermodynamic frameworks that can be applied to performance assessment for repositories in salt formations¹⁰ to include solubility limits and concomitant effects of aqueous solution complexation effects. The importance of obtaining accurate data and using consistent thermodynamic data to model them is obvious. For the aqueous solution this concerns the measurement of the proton activity, which is a master variable, and which is not trivial at high salt levels, and the calculation of correct activity coefficients¹¹.

Radionuclide retention due to surface reactions is typically represented in Performance Assessment calculations by the equilibrium distribution coefficient (K_d), which is a quotient between the adsorbed concentration of radionuclide (mass of radionuclide per unit mass of solid) and the aqueous concentration of radionuclide (mass of radionuclide per unit volume of solution)¹². Overall, K_d values lump together various processes (e.g. surface complexation, ion-exchange, precipitation, co-precipitation, etc.) and do not provide appreciable insight into the retention mechanism. Alternatively, radionuclide retention processes can be assessed through

the use of surface complexation models. Such approach, based on the definition on a mechanistic reaction model, can represent a variety of retention reactions (equilibrium and kinetic). It has become highly desirable to approach adsorption in more concentrated solutions, covering intermediate (0.1-1 M) and high ionic strength (>1 M), by similar procedures. This involves collection of experimental data in a systematic way on a model system in a first step and a subsequent attempt to rationalize the data in terms of a surface complexation model. As a model surface, quartz is studied in this work. Quartz presents well-known surface properties, with surface functional groups also present on the surface of clays and clay minerals. On the other hand, trivalent lanthanides, and more precisely, Eu has been selected as adsorbing solute of interest for the adsorption studies. This trivalent lanthanide cation is often used as a proxy for the radionuclides Am and Cm, which constitute an important fraction of the minor lanthanides/actinides present in the high-level liquid waste generated during the reprocessing of spent nuclear fuel¹³. In the scenario of a repository failure, these radionuclides could migrate away from the waste disposal site, finally entering the geosphere. During this migration process they will be interacting with the surrounding host-rock minerals. Consequently, a reliable understanding of their behaviour in contact with surfaces is crucial whenever retention processes are to be taken advantage of in the Safety Case for a given repository. Extensive studies have been carried out on the uptake of trivalent actinides onto mineral surfaces under different conditions¹³⁻¹⁸, but a study for high salt content on silica minerals is missing. In Germany and some other countries (Canada, USA, etc.) some options for repositories in areas that would involve highly saline aqueous solutions have been discussed and experimental data and models for treating such systems are required.

It is expected that such a model can be applied in Performance Assessment for a nuclear waste repository in highly saline environment in a similar way as is nowadays envisaged or applied for sorption from low ionic strength solutions in the licensing process for nuclear waste repositories or practised in general environmental contexts with respect to contaminant transport. Data on Eu adsorption on clay surfaces have been recently published up to high ionic strength and were modelled by a non-electrostatic surface complexation model coupled to the Pitzer approach¹⁶. While the coupling itself is rather a technical problem, the more interesting scientific issue is how traditional electrostatic models perform at high salt concentrations. One issue is whether coupled models yield a good fit to experimental data over the full range of background electrolyte content. Another arises from the fact that the application of the Gouy-Chapman-type treatment that is part of many of those models is beyond the limits of the underlying theory. For this reason, the constant capacitance model has been traditionally used as the equivalent of the constant ion medium approach in solution studies to treat the interfacial electrostatics at high - medium concentrations¹⁹. Although the constant capacitance model allows for variable ionic strength in a semi-predictive way²⁰, it is preferable to have a fully consistent set of surface complexation parameters to describe a given system. We therefore test a Basic Stern model to describe electrostatics at the mineral water interface up to high salt concentrations. Hiemstra

and co-workers⁹ modelled data on silica from Bolt²¹ up to 4M NaCl applying conventional activity corrections involving the Davies-equation. At the highest salt level, such approaches fail to correctly describe the activity corrections of the dissolved species. Except for the works of Schnurr et al.¹⁶ and Zoll and Schiff²², on clay minerals and algae respectively, we have no knowledge of a consistent treatment of the activity corrections up to salt brines in an adsorption study. This work therefore is the first attempt to couple Pitzer equations with an electrostatic model for the interface. The use of Pitzer equations to calculate activity coefficients at high ionic strength conditions is preferred because this model allows a robust description of the complex ion-interaction processes in saline media. As will be seen later, the model performs very well for our system. Furthermore, due to the high salt content, the impact of the Gouy-Chapman part (i.e. the diffuse part of the double layer) is of minor importance, since the fundamental charge caused by proton ad- and desorption from surface functional groups is sufficiently screened by counter-ion adsorption.

2. Materials and Methods

2.1 Materials

Commercially available MINUSIL 5 particles (pure quartz particles of nominal 5 μm size) were obtained from U.S. silica company. The solids were washed several times with dilute HNO_3 solutions, dried and checked for the absence of impurities by XPS. The XPS spectra (not shown) did not reveal any significant impurities on the pre-treated particles. The specific surface area (measured by BET using Nitrogen gas) of the pre-treated particles was 6.5 m^2/g .

2.2 Surface titrations and zeta potentials measurements

The MINUSIL solids were titrated at different NaCl concentrations (0.1, 1, 3 and 5M). Titrations were carried out in fast mode with small additions of titrant and short waiting times between additions. Calibration of the measurement set-up was done with standard procedure but considering the “A”-factor which allows to correct operational, measured pH values at high ionic strength to pH_c ($-\log[\text{H}^+]$)²⁰. The set-up was purged by purified and humidified Argon to avoid intrusion of carbon dioxide and limit evaporation. The data treatment followed standard procedures. The values for pK_w at the different ionic strengths were calculated using the Pitzer formalisms. The Pitzer parameters were those used by Schnurr et al.¹⁶ (for the Am-Na-Cl-system). They are self-consistent, and consistent between the treatment of the titration data and the modelling of our experimental titration and adsorption data. The raw data yielded the relative surface charge as a function of pH_c . For the modelling it is necessary to determine the absolute charge. It is not straightforward to decide how to treat the data at these high salt contents, as several pH-scales would be possible besides the pH_c scale. Plotting the relative data on any of these scales could yield a common intersection point. In the case of standard quartz no

common intersection point is expected, but the observed plateau down to low pH is usually set to absolute zero surface charge. Our data do not show classical quartz behaviour, therefore no clear acidity scale to define common intersection points can be defined. A consistent way to fix the absolute charge is to use the Pitzer pH scale within a model and involve zeta-potential measurements, which give an absolute value of the surface charge within the shear-plane. The DT-300 system from Quantachrome/Dispersion Technology was used for the electroacoustic experiments. Before each new measurement, a calibration of the probe is done in a particle-free solution, and the background current is automatically subtracted from the suspension measurements. Moreover, ultrasounds are applied for 3 min in the suspensions before any experiment using a sonotrode (UP100H model from Hielscher). To calculate zeta potential from electroacoustic measurements, a bimodal size distribution has been used, resulting from laser diffraction granulometry. The pH was measured in the usual way, i.e. by calibrating against three commercial buffers. With the lower ionic strength, no extra corrections were required.

2.3 Batch Sorption studies

Eu sorption onto MINUSIL particles was studied in NaCl solutions of different ionic strengths: 0.1, 1, 3 and 5M. The total concentration of Eu in all cases was $1 \cdot 10^{-7}$ M, the solid to liquid ratio was 10g/L, and pH_c values were varied in the range from 2.5 to 8.0 by HCl and NaOH solutions. The pH_c values were determined using the known “A”-factors as described in the previous section.

2.4 Speciation calculations and surface complexation modelling

Thermodynamic data ($\log \beta^0$ values) used in this work are identical to those used by Schnurr et al.¹⁶. We summarize the $\log \beta^0$ values for the aqueous Eu-species, which have been taken from the NEA compilation for Americium²³ (see Table 1). The Pitzer activity coefficients were used as indicated above. Europium and Americium, generally featuring analogous aqueous species with comparable structures, are usually treated within a common scheme to describe ion-interaction processes. The potential dissolution of quartz may result in the formation of silicic acid that may act as inorganic ligand for cations. However, in a related study it was found that addition of dissolved silica is required to affect the speciation in this system¹⁷. Moreover, increasing the system ionic strength largely decreases the stability of ternary aqueous species Eu-H₂O-Si. Thus, no attempt was made to include Si aqueous speciation in the model, i.e. ternary aqueous or surface species were not considered.

Table 1. $\log \beta^0$ used for calculating the aqueous speciation of Eu(III).

Reaction	$\log \beta^0$
$\text{Eu}^{3+} + \text{H}_2\text{O} \leftrightarrow \text{Eu}(\text{OH})^{2+} + \text{H}^+$	-7.20
$\text{Eu}^{3+} + 2\text{H}_2\text{O} \leftrightarrow \text{Eu}(\text{OH})_2^+ + 2\text{H}^+$	-15.1
$\text{Eu}^{3+} + 3\text{H}_2\text{O} \leftrightarrow \text{Eu}(\text{OH})_3(\text{aq}) + 3\text{H}^+$	-26.2
$\text{Eu}^{3+} + 4\text{H}_2\text{O} \leftrightarrow \text{Eu}(\text{OH})_4^- + 4\text{H}^+$	-40.6
$\text{Eu}^{3+} + \text{Cl}^- \leftrightarrow \text{EuCl}^{2+}$	0.24
$\text{Eu}^{3+} + 2\text{Cl}^- \leftrightarrow \text{EuCl}_2^+$	-0.74

Quartz surface protonation is modelled with a 2-site protolysis model ²⁴. The MINUSIL sample used in this study presents two distinct types of functional groups that govern the reactions taking place at the quartz surface. A basic Stern model is used for interfacial electrostatics of the system, which includes ion-specific effects via the formation of ion-pairs between ionized surface functional groups and ions of the background electrolyte ²⁵. For the fundamental charging the titration and zeta-potential results were fitted simultaneously. As previously explained, a major problem in the treatment of the titration data is that the absolute charge cannot be determined. Zeta-potentials are an absolute measure of the net-charge within the shear-plane and are affected by the proton ad- and desorption reactions. The coupling of the various data sets via UCODE is possible and allows the relative charging data obtained in the titrations ²⁶ to be transformed to absolute values, while simultaneously fitting capacitance and stability constants. Site densities were constrained as described below.

Metal ion adsorption is modelled by applying those parameters derived from titration results, i.e. capacitance and surface hydrolysis constants, and fitting a hypothetical surface complex stoichiometry with a charge distribution to the experimental Eu uptake data. Parameter fitting is done using the general parameter estimation software UCODE ²⁷ coupled to a modified version of FITEQL2 ²⁸.

No separate activity corrections apart from electrostatic factors are applied to the surface species, i.e. in the mass law equations for adsorption reactions only activity coefficients for dissolved species and activities of water are considered in the calculation of the ionic strength dependence of stability constants for surface species. The activity coefficients were separately calculated using the Pitzer formalism and available self-consistent databases, as described in detail elsewhere ¹⁶. The resulting activity coefficients were then used to calculate conditional stability constants at infinite dilution, or corrections factors to stability constants that were to be fitted. Fitting thus yields the stability constants at infinite dilution.

3. Results

3.1 Surface titrations and zeta potentials

Surface titration results are presented as symbols in Figure 1 in terms of surface charge (in $\text{mC}\cdot\text{m}^{-2}$) vs pH_c . The charging curves agree with some previously published studies²⁹, but only differ from the bulk of the literature data for quartz and silica, which show the deprotonation step at high pH. Our data are surprising in the sense that a distinct two step behaviour is observed. Usually such stepwise deprotonation is overshadowed by electrostatics and/or site distributions³⁰. Ong et al.²⁹ used second harmonic generation to study the interface between fused silica and sodium chloride solutions as a function of pH. They found a two step-behaviour and reported $\log \beta$ values of -4.5 and -8.5 in 0.5 M NaCl and a ratio of 1:4 between the two types of sites. There are various independent studies that report the existence of two distinct sites on various silica samples^{24,31–35}. Our proposed model involves two sites, as does the Ong et al. model, and Figure 1 and Figure 3 show the fits to the surface titrations and the zeta-potentials. Solid lines in Figure 1 represent the best fit results. The SCM parameters used in the fitting are detailed in Table 2. The site densities were constrained according to Ong et al. assuming a total site density of $4.6 \text{ sites}/\text{nm}^2$ ¹⁸.

In the acidic pH range ($\text{pH}_c < 6$), for the same pH_c value the negative surface charge increases when increasing the ionic strength of the system. A further decrease in the negative charge was observed in the basic pH range ($\text{pH}_c > 7$). This behaviour can be described by the speciation scheme presented in Figure 4. Deprotonated species are predominant in both, acidic and basic, pH_c conditions. We will refer to the more acidic site as the hydrophobic site x. Counter-ions (Na^+ and Cl^-) adsorption has also been considered (Table 2).

The pK_a values in our modelling have been placed close to those obtained by Ong et al. within a Diffuse Layer model for data at 0.5M NaCl²⁹. The site labelled y is the “usual” silanol site with an assigned pK value of about 8.5 and sodium association is also in the range typically reported^{13,17,29}. The “hydrophobic” site involves a pK value fixed at about 4.0. Overall, the two pK values for deprotonation extracted from our experimental data (i.e. 4.0 and 8.5) agree with independent data reported in the literature, i.e. 2-3 and 9-10 from³⁵, 4.5 and 8.5 from²⁹, 5.5 and 9.0 from³¹.

To be able to model the data we had to involve rather strong counter-ion association with the hydrophobic site. There have been recent reports on ion-specific effects on fused silica in the acidic range³⁶, which may be taken as support for our findings. A more direct indication from AFM measurements where the two sites were also identified on one sample shows that cation-specificity is inversed³⁷ and that the more acidic site is indeed showing the sequence expected for a hydrophobic surface³⁸.

Table 2. Parameters and reactions used to model the amphoteric behaviour of quartz surface with an electrostatic SCM model at infinite dilution. In italics fitted parameters.

Reaction	log <i>K</i> ⁰
$\equiv\text{Si}_x\text{OH} + \text{H}^+ \leftrightarrow \equiv\text{Si}_x\text{OH}_2^+$	-1.3 ^a
$\equiv\text{Si}_x\text{OH} \leftrightarrow \equiv\text{Si}_x\text{O}^- + \text{H}^+$	-4.0 ^b
$\equiv\text{Si}_y\text{OH} \leftrightarrow \equiv\text{Si}_y\text{O}^- + \text{H}^+$	-8.5 ^c
Parameter	
Site <i>x</i> (sites·nm ⁻²)	1.0
Site <i>y</i> (sites·nm ⁻²)	3.7
Capacitance (F·m ⁻²)	2.0
Specific surface area (m ² ·g ⁻¹)	6.5
Shear plane distance parameter ^d	0.03

a. Counter ion (Cl⁻) constant (log *K*) for $\equiv\text{Si}_x\text{OH}$ is 1.9; b. Counter ion (Na⁺) constant (log *K*) for $\equiv\text{Si}_x\text{OH}$ was 5.4; c. Counter ion (Na⁺) constant (log *K*) for $\equiv\text{Si}_y\text{OH}$ is 1.5. d. ratio between shear-plane distance and Debye-length; a value close to zero suggests that the model inherent shear-plane is close to the (theoretical) onset of the diffuse layer.

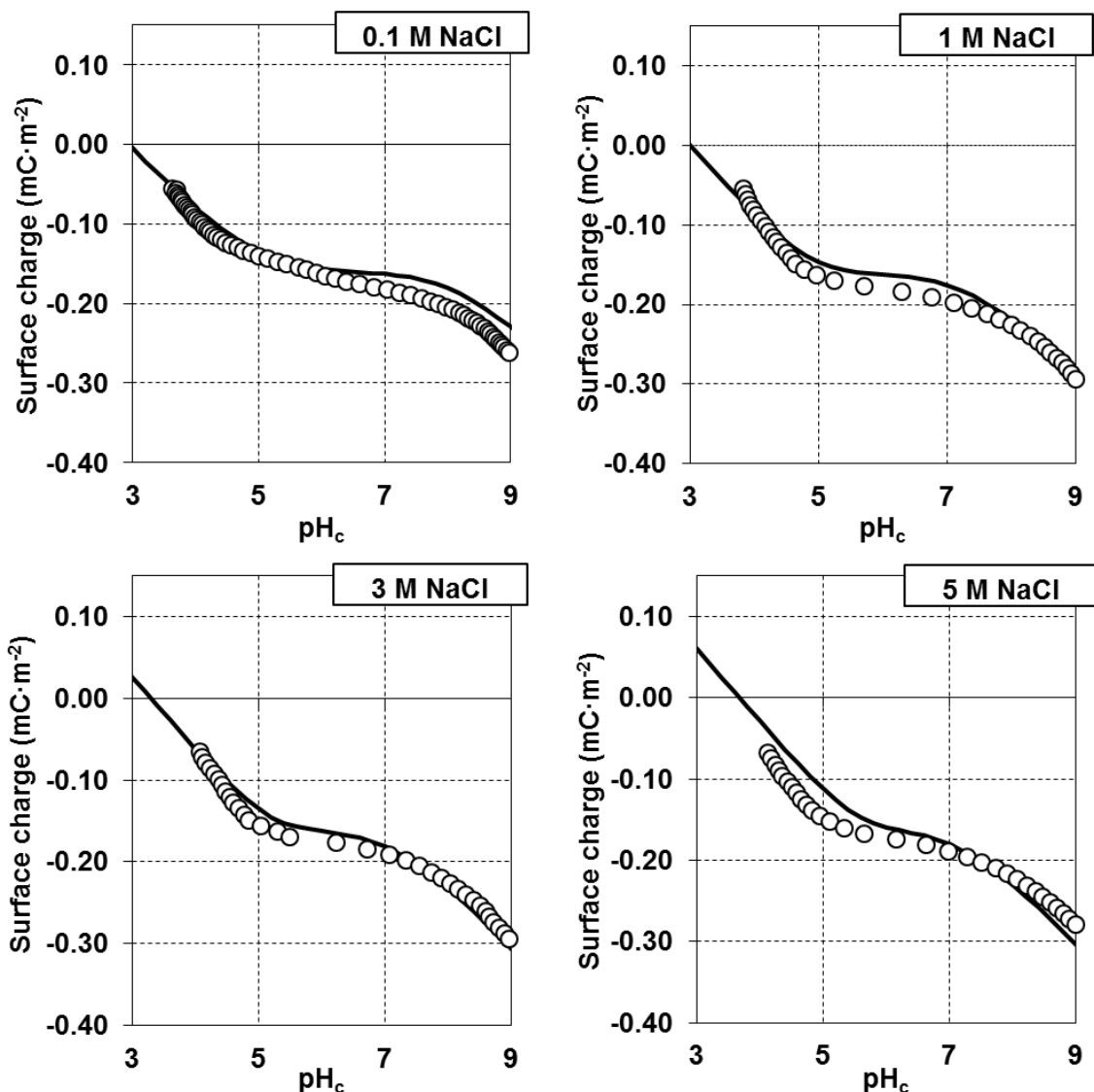


Figure 1. Surface charge density as a function of pH_c for MINUSIL quartz particles at different ionic strengths (0.1-5M) in NaCl medium. Symbols stand for the experimental results, while lines are the best fit model using Table 2 parameters and Pitzer activity coefficients for aqueous solution speciation.

A comparison between surface charge as a function of pH_c (concentration scale) respectively pH (activity scale, here Pitzer pH scale) is presented in Figure 2a and Figure 2b respectively. Figure 2 highlights that the mode of presenting the data (either on the concentration or on the activity scale) has some repercussion on how to classify the observations. On the concentration scale, there is strong effect of salt on the hydrophobic site, while there is no effect for the hydrophilic site at salt contents of 1M and above (Figure 2a). On the Pitzer-activity scale, hardly any effect of salt is observed on the hydrophobic site, while the hydrophilic site clearly follows the trend found in comparable studies at salt contents below 1M. The choice of the scales also has repercussions on how to classify specific adsorption as will be discussed later.

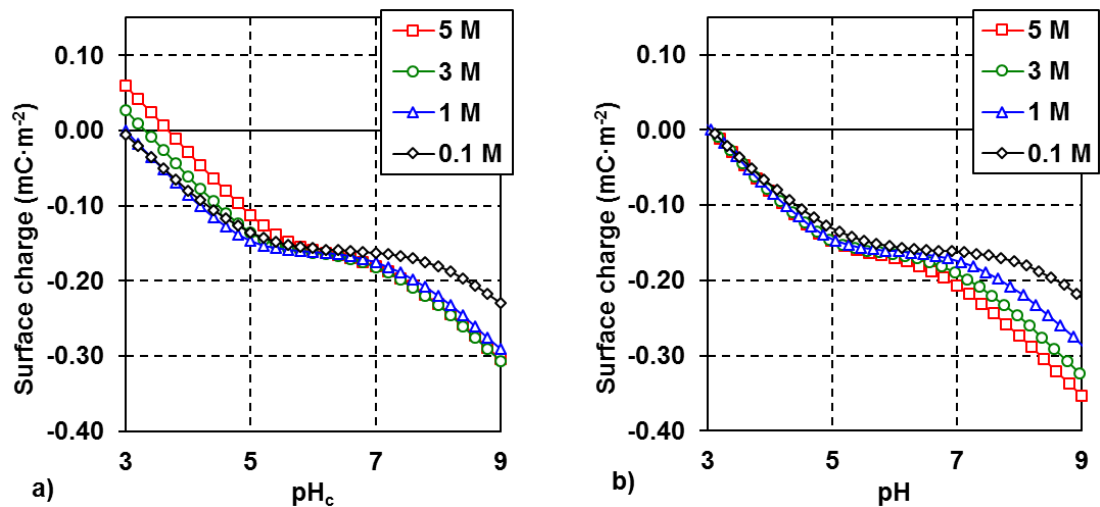


Figure 2. Calculated surface charge density as a function of a) pH_c and b) pH (Pitzer pH scale) for MINUSIL quartz particles at different ionic strengths (0.1-5M) in NaCl medium. Table 2 parameters and Pitzer activity coefficients for aqueous solution speciation have been used in these calculations.

282

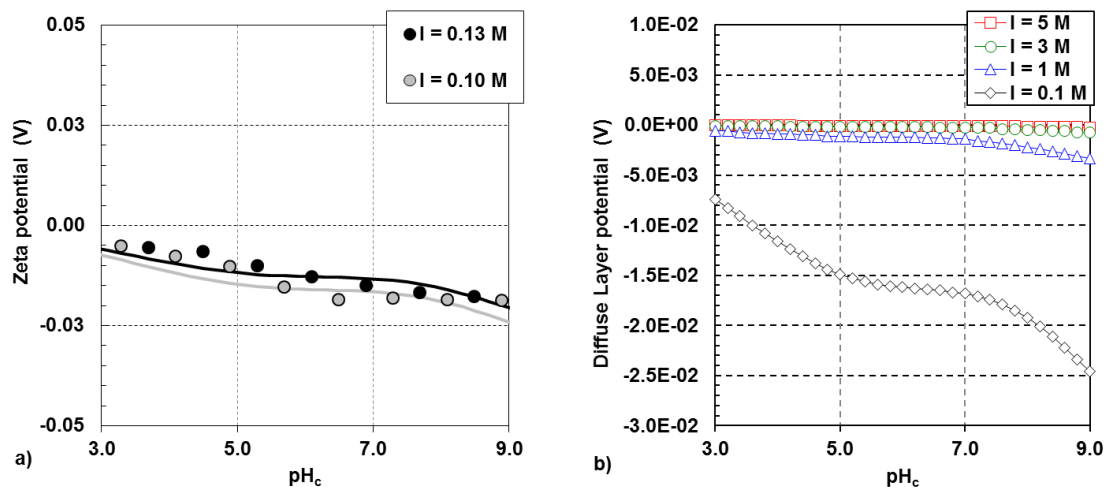


Figure 3. a) Zeta potentials as a function of pH_c for two different NaCl concentrations, 0.1 and 0.13M. Symbols stand for experimental data while lines are the predictions by the SCM detailed in Table 2. b) Diffuse Layer potentials as a function of pH_c for the different NaCl concentrations, from 0.1 to 5M, studied in the present work.

287

Figure 3 shows calculated interfacial potentials based on the present model. Figure 3a presents the measured zeta-potentials for the sample at approximately 0.1M NaCl with the concomitant model calculations, showing a rather good fit. Figure 3b shows the model inherent diffuse layer potentials for the various NaCl concentrations used in the titrations. Due to the strong ion-

pairing there is a strong drop in the interfacial potential up to the head end of the diffuse layer. The diffuse layer potentials become very low for $I \geq 1\text{ M NaCl}$. This justifies the application of the conventional diffuse layer, mainly because the diffuse layer potential becomes insignificant. The zeta-potentials can be described by a shear-plane distance parameter close to zero, which means the shear plane is nearly identical with the head end of the diffuse layer. Figure 4 shows the surface speciation according to the model for 0.1M (Figure 4 - a) and 5M (Figure 4 - b). The high salt content clearly drives the ion-pairs with sodium to control the speciation on the hydrophilic site.

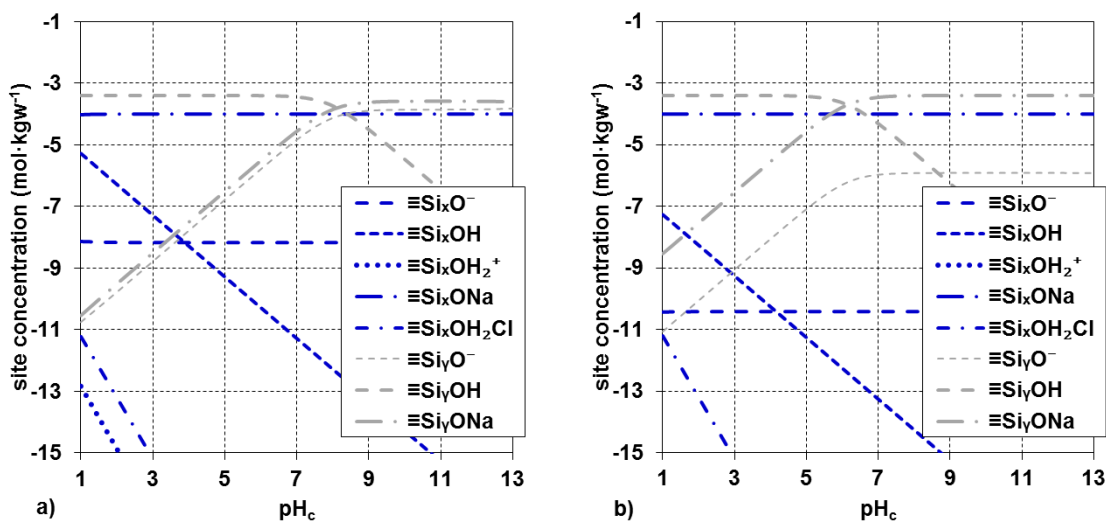


Figure 4. Silica surface speciation as a function of pH_c according with the model presented in Table 2, at a) 0.1M NaCl and b) 5.0M NaCl.

3.2 Aqueous speciation of Eu

Aqueous Eu speciation over a wide range of pH_c is shown in Figure 5 for the different NaCl concentrations. Increasing the ionic strength has not an important effect under acid conditions. The two aqueous species, EuCl^{2+} and EuCl_2^+ , are negligible even at Cl concentrations as high as 5M (not shown in the Figure). In the basic pH range ($\text{pH}_c > 8$), within our speciation scheme, minor differences can be observed with the increase of ionic strength. As pointed out by Schnurr et al.¹⁶, the Pitzer parameters for the chloride complexes in NaCl systems are not complete, but the resulting effects on europium speciation are minor.

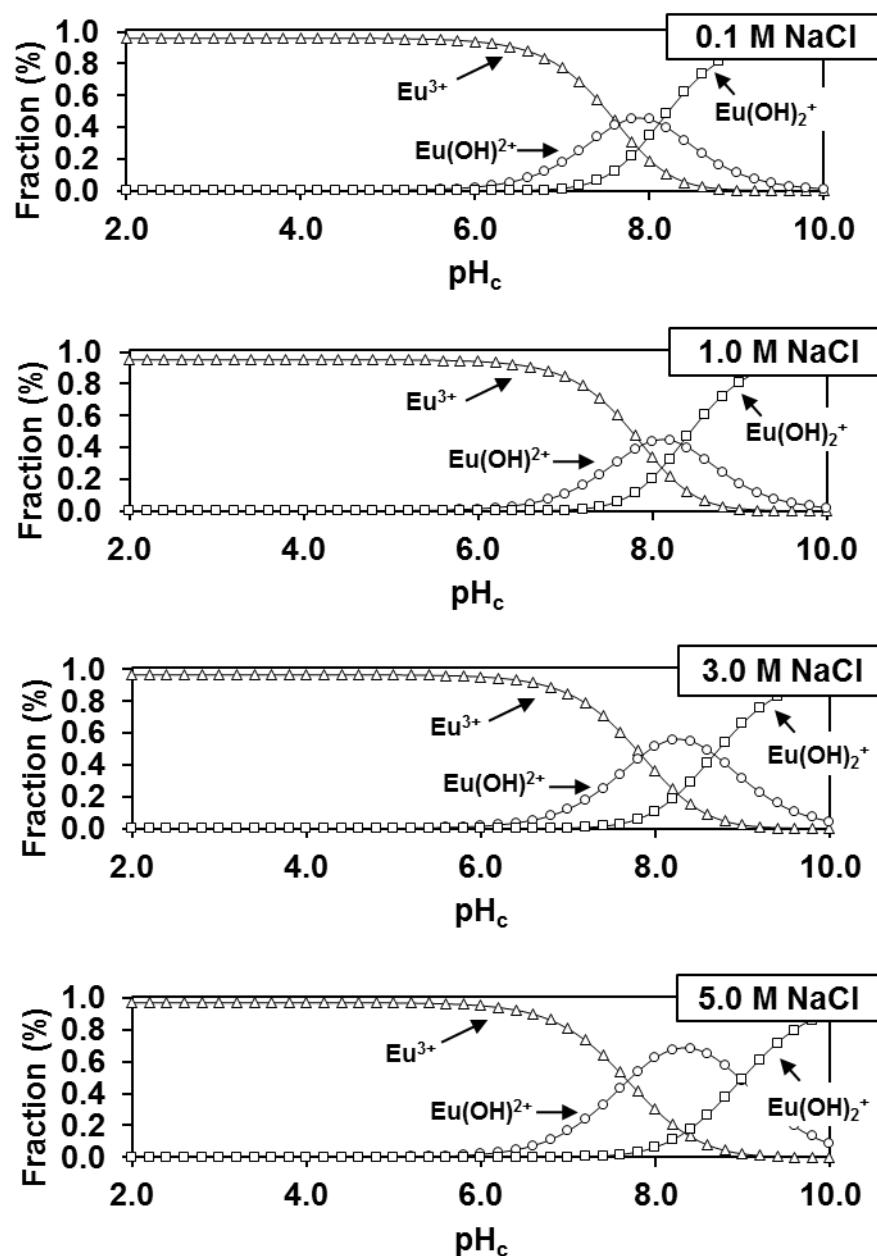


Figure 5. Aqueous speciation of Eu vs. pH_c based on the available thermodynamic parameters. Fraction of Eu species at different NaCl concentrations for $[\text{Eu}]_T = 1 \cdot 10^{-7} \text{ M}$. Thermodynamic data are reported in Table 1.

A more interesting feature in Figure 5 is that with increasing salt content, the model predicts a consistent increase in the stability of the first hydrolysis species over the other species. Clearly this species increases from below 50 % (at 0.1M) to almost 70 % (at 5M) of the total Eu in solution at 5M NaCl. The first hydrolysis species has often been considered relevant for the onset of adsorption³⁹, and linear free energy relationships are often used to relate surface complexation constants with the first hydrolysis constant in the case of cations. This would suggest stronger adsorption of Eu in the 0.1M NaCl system at a given pH_c compared to the higher ionic strengths.

3.3 Adsorption of Eu onto MINUSIL particles

Experimentally obtained Eu sorption edges are presented in Figure 6 (symbols) as fractional uptake vs pH_c in the various NaCl media (from 0.1 to 5 M). A shift in the sorption edges to higher pH_c is found on the log proton concentration (pH_c) scale with increasing ionic strength. In the four studied ionic strengths Eu adsorption onto quartz starts at $\text{pH}_c \sim 4$ and reaches almost 95% at $\text{pH}_c \sim 6$. At more basic conditions, nearly complete uptake is observed. As expected based on the aqueous speciation, enhanced adsorption is observed at the low pH_c in 0.1M NaCl compared to the higher ionic strengths.

The electrostatic SCM developed for simulating Eu uptake onto quartz by using the surface protonation model and the Eu aqueous speciation described above includes two bidentate surface complexes (Table 3). The stoichiometry was taken from Stumpf et al.¹⁷ and the stability constants have been fitted to the basic (i.e. classical silanol) site. No adsorption on the hydrophobic site was considered. This agrees with the recently reported cation adsorption sequence³⁷. Charge Distribution (CD) is applied in the SCM and CD factors are optimized as well. Model results are shown as solid lines in Figure 6, and show very good agreement with the experimental results.

Table 3. Parameters and reactions used to model Eu sorption onto quartz surface with an electrostatic SCM model at infinite dilution. The fitted parameters are given in italics. The charge distribution is given in terms of the charge of the Europium charge that is allocated to the surface plane.

Reaction	$\log K^0$	$\Delta z_{0,\text{Eu}}$
$2(\equiv\text{Si}_y\text{OH}) + \text{Eu}^{3+} \leftrightarrow 2(\equiv\text{Si}_y\text{O})\text{HEu}^{2+} + \text{H}^+$	<i>-0.65</i>	<i>0.36</i>
$2(\equiv\text{Si}_y\text{OH}) + \text{Eu}^{3+} + \text{H}_2\text{O} \leftrightarrow 2(\equiv\text{Si}_y\text{O})\text{EuOH}^+ + 2\text{H}^+$	<i>-10.02</i>	<i>0.02</i>

As pointed out above, in previous work¹⁷ the same bidentate model in terms of stoichiometry was already used to describe Am(III) and Cm(III) sorption onto another quartz sample. The authors at the time confirmed the presence of at least two Eu surface complexes on the quartz surface by means of TRLFS measurements and the TRLFS also suggested the applied proton stoichiometry in going from the first to the second surface complex. Differences in the model concepts and parameters, e.g. the use of Pitzer instead of Davies for activity corrections, or in the model parameters, e.g. system capacitance, silica surface protonation, CD factors explain the observed discrepancies in model parameters between the study of Stumpf et al. and ours. Considering the CD-factors, the present results indicate a more outer-sphere-type surface complex formation for the same overall stoichiometry compared to Stumpf et al.¹⁷. In a more recent work, Kar and Tomar¹³ modelled Cm(III) sorption onto silica at 0.1M NaCl and reported the formation of two distinct monodentate surface complexes, $\equiv\text{SiOCm}^{2+}$ and $\equiv\text{SiOCm}(\text{OSi}(\text{OH})_3)_2$, with log K of -2.53 and -7.94 respectively. These authors applied a Diffuse

Layer Model (DLM) for describing the interfacial electrostatics of the system. The formation of the ternary aqueous species $\text{Cm-H}_2\text{O-Si, } \equiv\text{Si}_x\text{OCm(OSi(OH)}_3)_2$ as in the study Kar and Tomar, was not pursued in the present work, since no Pitzer parameters are available for the silica system. It has already been mentioned that Stumpf et al. reported no effect on the uptake and the spectroscopic results when adding dissolved silica to the Cm/quartz particle systems. Only when the silica concentration was raised to concentrations as high as 10 mM a significant effect was observed with quartz single crystals. The observations by Stumpf et al. are not necessarily proof for the absence of ternary silicato surface complexes in our study. Yet, the shift in the TRLFS spectra from species 1 to 2 is very similar to that observed for other oxide systems, where no ternary surface complexes were suspected⁴⁰.

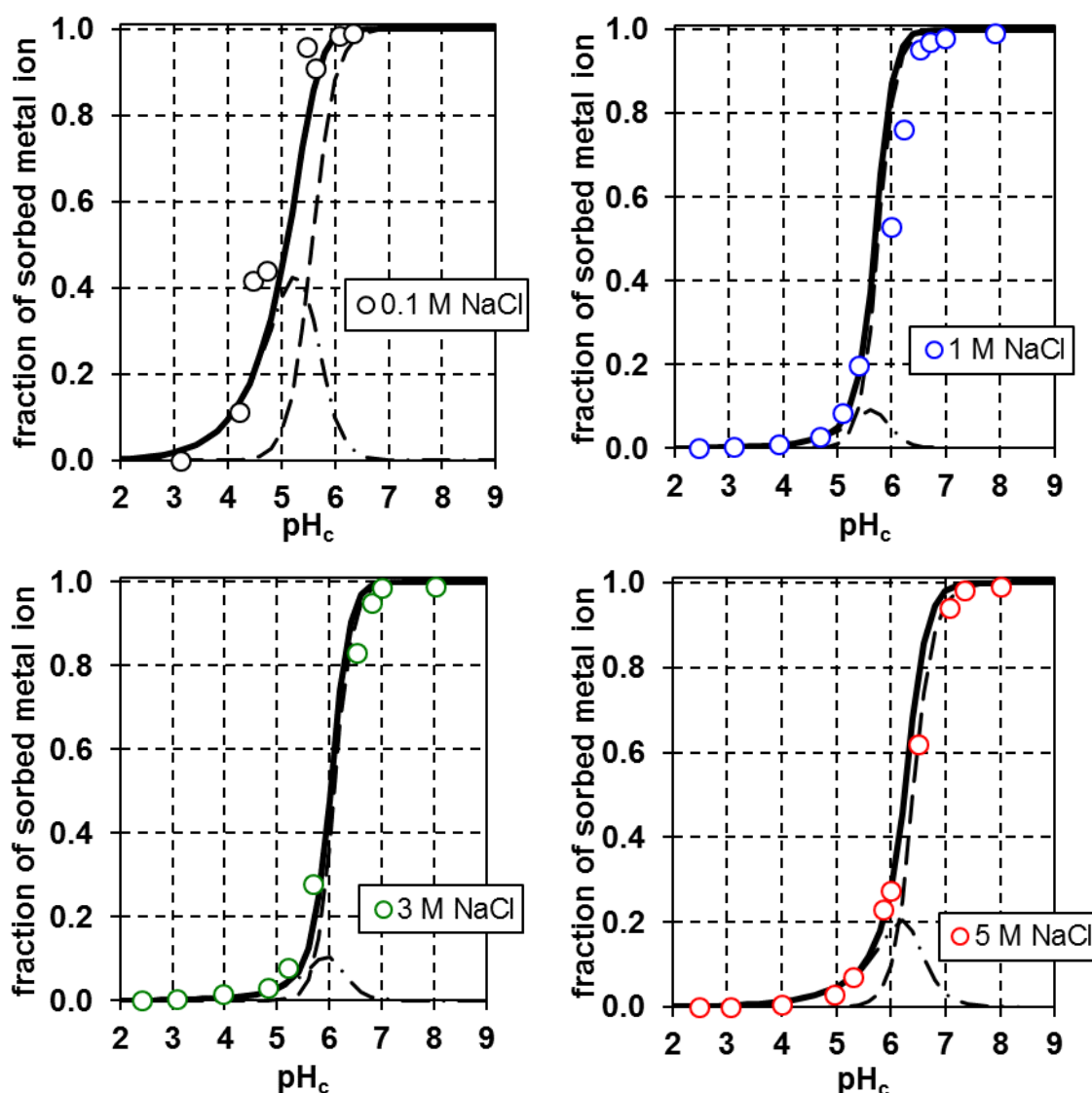


Figure 6. Fractional uptake of Eu ($[\text{Eu}]_{\text{T}}=1 \cdot 10^{-7}\text{M}$), S/L 10g/L, on MINUSIL as a function of pH_c and at different NaCl concentrations. Experimental data are given by symbols. Solid lines are calculations using the sub-system parameters (Tables 1 and 2) and the SCM summarized in Table 3 involving Pitzer activity coefficients for aqueous solution speciation. Dashed lines

represent the calculated contribution of $2(\equiv\text{Si}_y\text{O})\text{HEu}^{2+}$ while dashed dotted lines stand for the contribution of $2(\equiv\text{Si}_y\text{O})\text{EuOH}^{2+}$ according to our SCM results.

Overall, it is concluded that the proposed model is able to describe the surface charge and Eu-uptake data up to 5M NaCl concentrations. As in the case of the titrations, Figure 7 highlights that the mode of presenting the data has some repercussion on how to classify the observations. On the concentration scale, a clear shift in the sorption edges to higher pH_c is found with increasing ionic strength (Figure 7a). On the Pitzer-activity scale, such a trend cannot be clearly observed for salt contents of 1M and above (Figure 7b).

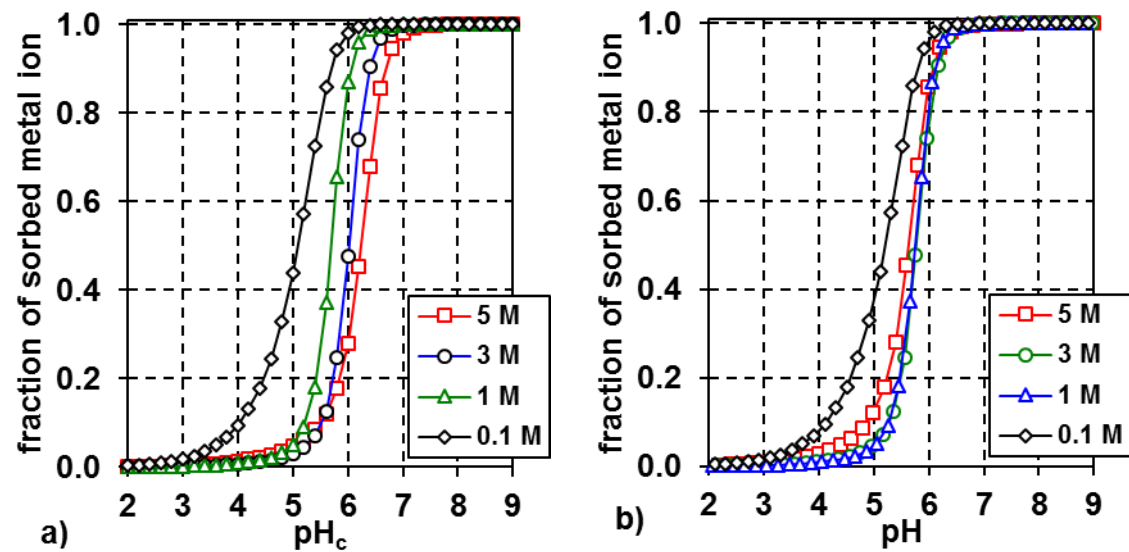


Figure 7. Predicted sorption edges for Eu ($[\text{Eu}]_{\text{T}}=1\cdot10^{-7}\text{M}$), S/L 10g/L, on MINUSIL as a function of a) pH_c and b) pH (Pitzer pH scale) at different NaCl concentrations. Predictions obtained with Table 2 - Table 3 parameters and Pitzer activity coefficients for aqueous solution speciation.

4. Conclusions

In the present study, the amphoteric quartz surface behaviour as well as the adsorption of Eu(III) onto quartz surface were reported up to high ionic strengths of 5M in NaCl. An electrostatic surface complexation model has been designed to describe the acid-base, zeta-potential and Eu(III) uptake data in a comprehensive, self-consistent way We obtained the following results:

- The titration of the quartz sample showed the clear presence of two sites from dilute to concentrated conditions.
- The salinity effects on quartz surface charge density can be described in different ways depending on the pH scale chosen. On the concentration scale a major effect occurs at acid pH conditions, while on the activity scale, the effect at low pH is absent.

-The presence of the two sites and their concomitant surface protonation within the model developed in this work is in fair agreement with previously published models covering lower ionic strength conditions for quartz showing similar behaviour.

-Within the model, at high ionic strength ($I > 1\text{M}$), the surface potential is strongly screened by ion-pair formation and the diffuse layer potential is negligibly low, which justifies the extension of the standard electrostatic model to the highly saline conditions.

-Eu(III) sorption edges onto quartz shift towards higher pH_c with increasing ionic strength, as expected based on the Eu(III) hydrolysis behaviour. As for the charging data, the chosen pH scale affects the observation or not of an ionic strength effect on Eu(III) uptake.

-A charge distribution SCM has been fitted to the Eu(III) adsorption data involving two bidentate Eu surface species.

-The proposed new model is in agreement with previous studies at low ionic strength conditions¹⁷, but the derived $\log K$ values differ somewhat probably related to the CD-factors and related to the presence of the hydrophobic site.

-Coupling a Pitzer approach for the aqueous phase to a conventional surface complexation model is fairly successful in describing the experimental data even when an electrostatic model is used.

-Trivalent lanthanide uptake will be of significant importance even in solutions of high ionic strengths.

-The model approach applied in this work can contribute to the Safety Case for nuclear waste repositories in formations potentially involving high salt content.

Acknowledgements

Authors acknowledge funding from ACTINET-I3 project – Contract Number: 232631.

References

- (1) Bradbury, M. H.; Baeyens, B. A General Application of Surface Complexation to Modeling Radionuclide Sorption in Natural Systems. *J. Colloid Interface Sci.* **1993**, *158* (2), 364–371.
- (2) Lützenkirchen, J. Summary of Studies on (Ad) Sorption as a “Well-Established” Process within FUNMIG Activities. *Appl. Geochem.* **2012**, *27* (2), 427–443.
- (3) Davis, J. A.; Kent, D. B. Mineral-Water Interface Geochemistry; Hochella, F. F., White, A. F., Eds.; Mineralogical Society of America, 1990; pp 177–260.
- (4) Dzombak, D. A.; Morel, F. M. M. *Surface Complexation Modelling: Hydrous Ferric Oxide*; Sons, J. W. &, Ed.; Wiley-Interscience, 1990.
- (5) Karamalidis, A. K.; Dzombak, D. A. *Surface Complexation Modelling: Gibbsite*; John Wiley & Sons, 2011.
- (6) Lützenkirchen, J. *Surface Complexation Modelling*; Academic Press, 2006; Vol. 11.
- (7) Mahoney J.J.; Langmuir D. Adsorption of Sr on Kaolinite, Illite and Montmorillonite at High Ionic Strengths. *Radiochim. Acta* **1991**, *54* (3), 139. <https://doi.org/10.1524/ract.1991.54.3.139>.
- (8) Rafferty, P.; Shiao, S.-Y.; Binz, C. M.; Meyer, R. E. Adsorption of Sr(II) on Clay Minerals: Effects of Salt Concentration, Loading, and PH. *J. Inorg. Nucl. Chem.* **1981**, *43* (4), 797–805. [https://doi.org/10.1016/0022-1902\(81\)80224-2](https://doi.org/10.1016/0022-1902(81)80224-2).

- 447 (9) Hiemstra, T.; De Wit, J. C. .; Van Riemsdijk, W. . Multisite Proton Adsorption Modelling
448 at the Solid/Solution Interface of (Hydr)Oxides: A New Approach: II. Application to
449 Various Important (Hydr)Oxides. *J. Colloid Interface Sci.* **1989**, *133* (1), 105–117.
450 [https://doi.org/http://dx.doi.org/10.1016/0021-9797\(89\)90285-3](https://doi.org/http://dx.doi.org/10.1016/0021-9797(89)90285-3).
- 451 (10) Reed, D. T.; Clark, S. B.; Rao, L. *Actinide Speciation in High Ionic Strength Media:
452 Experimental and Modelling Approaches to Predicting Actinide Speciation and Migration
453 in the Subsurface*; Springer Science & Business Media, 1999.
- 454 (11) Altmaier, M.; Metz, V.; Neck, V.; Müller, R.; Fanghänel, T. Solid-liquid equilibria of
455 $\text{Mg}(\text{OH})_2(\text{cr})$ and $\text{Mg}_2(\text{OH})_3\text{Cl}\cdot 4\text{H}_2\text{O}(\text{cr})$ in the system $\text{Mg}-\text{Na}-\text{H}-\text{OH}-\text{Cl}-\text{H}_2\text{O}$ at 25°C
456 <https://www.sciencedirect.com/science/article/pii/S0016703703001650> (accessed Mar
457 5, 2019).
- 458 (12) Domènech, C.; García, D.; Pekala, M. Decreasing K_d uncertainties through the
459 application of thermodynamic sorption models
460 <https://www.sciencedirect.com/science/article/pii/S0048969715300292> (accessed Mar
461 5, 2019).
- 462 (13) Kar, A. S.; Tomar, B. S. Cm(III) Sorption by Silica: Effect of Alpha Hydroxy Isobutyric Acid.
463 *Radiochim. Acta* **2014**, *102* (9), 763–773.
- 464 (14) Alliot, C.; Bion, L.; Mercier, F.; Toulhoat, P. Effect of Aqueous Acetic, Oxalic, and
465 Carbonic Acids on the Adsorption of Europium (III) onto α -Alumina. *J. Colloid Interface
466 Sci.* **2006**, *298* (2), 573–581.
- 467 (15) Kar, A. S.; Tomar, B. S.; Godbole, S. V.; Manchanda, V. K. Time Resolved Fluorescence
468 Spectroscopy and Modelling of Eu(III) Sorption by Silica in Presence and Absence of
469 Alpha Hydroxy Isobutyric Acid. *Colloids Surf. Physicochem. Eng. Asp.* **2011**, *378*, 44–49.
470 <https://doi.org/http://dx.doi.org/10.1016/j.colsurfa.2011.01.039>.
- 471 (16) Schnurr, A.; Marsac, R.; Rabung, T.; Lützenkirchen, J.; Geckeis, H. Sorption of Cm (III)
472 and Eu (III) onto Clay Minerals under Saline Conditions: Batch Adsorption, Laser-
473 Fluorescence Spectroscopy and Modelling. *Geochim. Cosmochim. Acta* **2015**, *151*, 192–
474 202.
- 475 (17) Stumpf, S.; Stumpf, T.; Lützenkirchen, J.; Walther, C.; Fanghänel, T. Immobilization of
476 Trivalent Actinides by Sorption onto Quartz and Incorporation into Siliceous Bulk:
477 Investigations by TRLFS. *J. Colloid Interface Sci.* **2008**, *318* (1), 5–14.
478 <https://doi.org/http://dx.doi.org/10.1016/j.jcis.2007.09.080>.
- 479 (18) Takahashi, Y.; Murata, M.; Kimura, T. Interaction of Eu(III) Ion and Non-Porous Silica:
480 Irreversible Sorption of Eu(III) on Silica and Hydrolysis of Silica Promoted by Eu(III). *J.
481 Alloys Compd.* **2006**, *408–412* (0), 1246–1251.
482 <https://doi.org/http://dx.doi.org/10.1016/j.jallcom.2005.04.120>.
- 483 (19) Schindler, P. W.; Gamsjager, H. Acid - Base Reactions of the TiO_2 (Anatase) - Water
484 Interface and the Point of Zero Charge of TiO_2 Suspensions. *Kolloid-Z. Z. Polym.* **1972**,
485 *250* (7), 759–763. <https://doi.org/10.1007/BF01498568>.
- 486 (20) Lützenkirchen, J. The Constant Capacitance Model and Variable Ionic Strength: An
487 Evaluation of Possible Applications and Applicability. *J. Colloid Interface Sci.* **1999**, *217*
488 (1), 8–18. <https://doi.org/http://dx.doi.org/10.1006/jcis.1999.6348>.
- 489 (21) Bolt, G. H. Determination of the Charge Density of Silica Sols. *J. Phys. Chem.* **1957**, *61*
490 (9), 1166–1169. <https://doi.org/10.1021/j150555a007>.
- 491 (22) Zoll, A. M.; Schifj, J. A surface complexation model of YREE sorption on *Ulva lactuca* in
492 0.05–5.0 M NaCl solutions
493 <https://www.sciencedirect.com/science/article/pii/S0016703712004802?via%3Dihub>
494 (accessed Mar 5, 2019).
- 495 (23) Guillaumont, R.; Fanghänel, T.; Fuger, J.; Grenthe, I.; Neck, V.; Palmer, D. A.; Rand, M. H.
496 *Chemical Thermodynamics 5: Update on the Chemical Thermodynamics of Uranium,
497 Neptunium, Plutonium, Americium and Technetium*; V. N. N. H. E. S. P. B., Ed.; 2003.

- 498 (24) Sverjensky, D. A.; Sahai, N. Theoretical Prediction of Single-Site Surface-Protonation
499 Equilibrium Constants for Oxides and Silicates in Water. *Geochim. Cosmochim. Acta*
500 **1996**, 60 (20), 3773–3797. [https://doi.org/http://dx.doi.org/10.1016-](https://doi.org/http://dx.doi.org/10.1016/0016-7037(96)00207-4)
501 7037(96)00207-4.
- 502 (25) Kulik, D. Thermodynamics and Kinetics of Water-Rock Interactions; Oelkers, E. H.,
503 Schott, J., Eds.; Mineralogical Society of America, 2009; pp 125–180.
- 504 (26) Lützenkirchen, J.; Preočanin, T.; Kovačević, D.; Tomišić, V.; Lövgren, L.; Kallay, N.
505 Potentiometric Titrations as a Tool for Surface Charge Determination. *Croat. Chem. Acta*
506 **2012**, 85 (4), 391–417.
- 507 (27) Poeter, E. P.; Hill, M. C. *Documentation of UCODE: A Computer Code for Universal*
508 *Inverse Modelling*, DIANE Publishing.; 1998.
- 509 (28) Westall, J. C. *FITEQL: A Computer Program for Determination of Chemical Equilibrium*
510 *Constants from Experimental Data*; Department of Chemistry, Oregon State University,
511 1982.
- 512 (29) Ong, S.; Zhao, X.; Eiseenthal, K. B. Polarization of Water Molecules at a Charged
513 Interface: Second Harmonic Studies of the Silica/Water Interface. *Chem. Phys. Lett.*
514 **1992**, 191, 327–335. [https://doi.org/http://dx.doi.org/10.1016/0009-2614\(92\)85309-X](https://doi.org/http://dx.doi.org/10.1016/0009-2614(92)85309-X).
- 515 (30) Lützenkirchen, J. On Derivatives of Surface Charge Curves of Minerals. *J. Colloid*
516 *Interface Sci.* **2005**, 290 (2), 489–497.
517 <https://doi.org/http://dx.doi.org/10.1016/j.jcis.2005.04.074>.
- 518 (31) Allen, L. H.; Matijević, E.; Meites, L. Exchange of Na⁺ for the Silanolic Protons of Silica. *J.*
519 *Inorg. Nucl. Chem.* **1971**, 33 (5), 1293–1299.
- 520 (32) Branda, M. M.; Montani, R. A.; Castellani, N. J. The Distribution of Silanols on the
521 Amorphous Silica Surface: A Monte Carlo Simulation. *Surf. Sci.* **2000**, 446 (1–2), L89–
522 L94. [https://doi.org/http://dx.doi.org/10.1016/S0039-6028\(99\)01133-4](https://doi.org/http://dx.doi.org/10.1016/S0039-6028(99)01133-4).
- 523 (33) Krasnansky, R.; Thomas, J. K. Aminopyrene as a Monitor of Vicinal and Geminal OH
524 Groups on Silica. *Langmuir* **1994**, 10 (12), 4551–4553.
- 525 (34) Murray, D. K. Differentiating and Characterizing Geminal Silanols in Silicas by ²⁹Si NMR
526 Spectroscopy. *J. Colloid Interface Sci.* **2010**, 352 (1), 163–170.
527 <https://doi.org/http://dx.doi.org/10.1016/j.jcis.2010.08.045>.
- 528 (35) Pfeiffer-Laplaud, M.; Costa, D.; Tielens, F.; Gaigeot, M.-P.; Sulpizi, M. The Bi-Modal
529 Acidity at the Amorphous Silica/Water Interface. *J. Phys. Chem. C* **2015**.
- 530 (36) Azam, M. S.; Darlington, A.; Gibbs-Davis, J. M. The Influence of Concentration on
531 Specific Ion Effects at the Silica/Water Interface. *J. Phys. Condens. Matter* **2014**, 26 (24),
532 244107.
- 533 (37) Morag, J.; Dishon, M.; Sivan, U. The Governing Role of Surface Hydration in Ion Specific
534 Adsorption to Silica: An AFM-Based Account of the Hofmeister Universality and Its
535 Reversal. *Langmuir* **2013**, 29 (21), 6317–6322. <https://doi.org/10.1021/la400507n>.
- 536 (38) Lützenkirchen, J. Specific Ion Effects at Two Single-Crystal Planes of Sapphire. *Langmuir*
537 **2013**, 29 (25), 7726–7734. <https://doi.org/10.1021/la401509y>.
- 538 (39) James, R. O.; Healy, T. W. Adsorption of Hydrolyzable Metal Ions at the Oxide-Water
539 Interface. I. Co(II) Adsorption on SiO₂ and TiO₂ as Model Systems. *J. Colloid Interface Sci.*
540 **1972**, 40 (1), 42–52. [https://doi.org/http://dx.doi.org/10.1016/0021-9797\(72\)90172-5](https://doi.org/http://dx.doi.org/10.1016/0021-9797(72)90172-5).
- 541 (40) Geckeis, H.; Lützenkirchen, J.; Polly, R.; Rabung, T.; Schmidt, M. Mineral-Water Interface
542 Reactions of Actinides. *Chem. Rev.* **2013**, 113 (2), 1016–1062.
543 <https://doi.org/10.1021/cr300370h>.
- 544